Bio-Medical Materials and Engineering 26 (2015) S1125–S1133
DOI 10.3233/BME-151409
IOS Press

Nonholonomic mobile system control by combining EEG-based BCI with ANFIS

Weiwei Yu[a,*], Huashan Feng[a], Yangyang Feng[a], Kurosh Madani[b] and Christophe Sabourin[b]
[a]*School of Mechatronic Engineering, Northwestern Polytechnical University, Youyi Xilu 127hao, Xi'an, 710072, China*
[b]*Images, Signals and Intelligence Systems Laboratory (LISSI/EA 3956), UPEC University, Senart-Fontainebleau Institute of Technology, Bât.A, F-77127 Lieusaint, France*

Abstract. Motor imagery EEG-based BCI has advantages in the assistance of human control of peripheral devices, such as the mobile robot or wheelchair, because the subject is not exposed to any stimulation and suffers no risk of fatigue. However, the intensive training necessary to recognize the numerous classes of data makes it hard to control these nonholonomic mobile systems accurately and effectively. This paper proposes a new approach which combines motor imagery EEG with the Adaptive Neural Fuzzy Inference System. This approach fuses the intelligence of humans based on motor imagery EEG with the precise capabilities of a mobile system based on ANFIS. This approach realizes a multi-level control, which makes the nonholonomic mobile system highly controllably without stopping or relying on sensor information. Also, because the ANFIS controller can be trained while performing the control task, control accuracy and efficiency is increased for the user. Experimental results of the nonholonomic mobile robot verify the effectiveness of this approach.

Keywords: BCI, motor imagery EEG, ANFIS, nonholonomic mobile system

1. Introduction

BCI (Brain Computer Interface) technology is not only a result of human brain cognitive research, but can also further aid the control of peripheral equipment by replicating actions induced by human thought, inspiring promising application prospects in the biomedical and bioengineering domains. The subject suffers no risk of fatigue in the motor imagery paradigm, because there is no need for the subject to be exposed during the simulation process [1]. Therefore, ERD/ERS motor imagery EEG offers distinct advantages in the research of EEG-based control for peripheral devices, such as nonholonomic systems including the mobile robot and intelligent wheelchair.

Different protocols have been suggested for nonholonomic system control tasks based on motor imagery EEG. One example is the motor imagery BCI system developed by R. Leeb, in which the tetraplegic patient only imagines the movements of his paralyzed feet, one control command for a self-paced wheelchair control [2]. Other research has presnented easier ways to initiate more control commands. A previous study achieved the development of a robot which performed “turn left then

* Address for correspondence: Weiwei Yu, School of Mechatronic Engineering, Northwestern Polytechnical University, Youyi Xilu 127hao, Xi'an, 710072, China, Tel.: +86 18709243042; Fax: +86 29 88494271; E-mail: yuweiwei@nwpu.edu.cn.

move forward" or "turn right then move forward" in respond to two kinds of motor imagery EEG signals [3]. K. Choi developed the wheelchair, which could realize three motion behaviors: turning left, turning right and moving forward [1]. A 2-D virtual wheelchair controlled by ERD/ERS was designed by D. Huang, but its steering behavior is limited to forward movement, stop, right and left turn [4].

To increase the motion flexibility of the nonholonomic system, the motor imagery EEG-based hybrid BCI is proposed. This framework combines motor imagery EEG with other types of mental activity modalities or non-brain based activities systems, such as electromyogram or EOG. A hybrid BCI approach comprising motor imagery and P300 was previously designed by Y. Li, et al. [5]; acceleration and deceleration were determined by a joint feature composed of P300 and motor imagery EEG, to control both the direction and speed of a wheelchair [6]. This approach was further developed to utilize blinking of the eyes to achieve seven steering behaviors of a wheelchair; the forward, backward, right and left steering behaviors were determined by motor imagery, while stop was determined by eye-blinking [7]. A hybrid interface of eye movements and motor imagery EEG, which augments the number of control commands, was proposed to enable the flying robot to travel in eight different directions [8]. S. Bhattacharyya employed finger-elbow-shoulder movement classification in addition to arm movement classification to increase the motion freedom of a mobile robot. However, the complexity of the hybrid system necessitates more complex coding for extensive control [9].

A higher number of commands ease the mobile system's navigation through the environment. However, because the discrimination between different ERD/ERS patterns becomes more difficult with increasing class number, more command options may require more training. A classification error corresponds to a wrong control command, which can cause dangerous situations in the real world. Significant work has been done to match the number of commands to the number of mental tasks [10, 11]. For example, by incorporating motor imagery EEG with auditory BCI, F. Velasco-Álvarez operated only two mental tasks: relaxed state versus imagination of right hand movements to reduce the probability of misclassification [12]. Now four generally accepted common classes of ERD/ERS based EEG can be ensured for recognition and classification accuracy. Furthermore, the limited number of recognized control inputs makes the nonholonomic system stop frequently to achieve full direction maneuvers. J. Millan proposed the use of three classes of motor imagery EEG combined with an intelligent system to control a wheelchair; the results show the feasibility of continuously controlling complex robotic devices [13]. K.T. Kim presented a motor imagery based brain-actuated wheelchair system using an extended five command protocol: left, right, forward, left-diagonal, and right-diagonal, the smooth turning increasing the efficiency for the user [14].

In order to solve the limitations of control accuracy and frequent stopping, this paper proposes a new approach which combines motor imagery EEG with the Adaptive Neural Fuzzy Inference System (ANFIS). This approach may be segmented into two parts: the first one allows the mobile system to plan a "collision-free holonomic path" based on four classes of ERD/ERS EEG, and the second is composed of position and orientation controls based on ANFIS, allowing the nonholonomic mobile system to approximate the desired path. The advantage of this hybrid control system is that its execution mimics a human control mechanism; the motion planning process is accomplished by the brain and the implementing process is realized by a kind of "unconscious" biosome mechanism, as is the process of human leg movement.

2. Motion planning by motor imagery EEG

2.1. Signal acquisition

EEG signals are referentially recorded using Brain Products actiCHamp system with 32 electrodes placed on the subject's head: nine electrodes are related to imagery EEG data acquisition. The reference electrodes are mounted on the right and left ear. The sampling frequency rate is 500 Hz, and all electrode impedances are maintained below 5 kΩ. Taking into account that the subject needs to achieve right hand, left hand and foot movements accurately and promptly, we chose the subject who had previous experience driving a car (male, 28 years old).

2.2. Signal preprocessing, feature extraction and classification

The signal and noise disperse in the entire scalp and form diffuse noise, which results in a strong correlation between the electrodes. Linear combination of data from multiple EEG electrodes can effectively improve the signal to noise ratio. Because the signal and noise of an EEG have the characteristics of obvious spatial distribution, Common Average Reference (CAR) is chosen to reduce the correlation between electrodes.

Spatial patterns of motor imagery EEG are calculated by one versus rest (OVR) common spatial patterns (CSP) computationally [15], this method is parallel to nature and requires only scalar products. Therefore, it is optimal for real-time applications.

The linear Support Vector Machine (SVM) is used to classify the feature vectors obtained from EEG signals into each class of motor imagery. The SVM constructs a hyperplane in high-dimensional space for classification. Each hyperplane separates the training data point of any class with the largest possible margin.

3. Trajectory tracking for nonholonomic mobile system by ANFIS

3.1. Nonholonomic mobile system

A mobile system is said to be nonholonomic when the dimension of the configuration space is greater than the number of controls [16].

$$\begin{cases} \dot{x} = \dfrac{1}{2}(R\omega_r + R\omega_l)\cdot\cos\theta \\ \dot{y} = \dfrac{1}{2}(R\omega_r + R\omega_l)\cdot\sin\theta \\ \dot{\theta} = \dfrac{1}{2L}(R\omega_r - R\omega_l) \end{cases} \tag{1}$$

For example, a two-wheeled robot or a wheelchair's kinematic model can be expressed as Eq. (1), where ω_r and ω_l are the actuating speeds of the right and left wheel respectively, r denotes radius of wheel and L denotes span. θ represents the angle between the longitudinal axes of the robot and the coordinate system. The configuration space can be expressed by (x, y, θ), which is in 3-dimensions and the number of controlled dimensions limit to two.

3.2. ANFIS controller for nonholonomic mobile system

The path planning produced by a limited number of motor imagery EEG-based control commands is only viable for holonomic systems. In order to execute continuous maneuvers, the controller of the nonholonomic mobile system has to accomplish two functions: first, approximate a collision-free holonomic path in order to find a reference path feasible for the nonholonomic system. Secondly, track the reference path by controlling the position and orientation of the object.

3.2.1. Approximation for trajectory of holonomic mobile system

Motor imagery EEG is acquired and classified according to Section 2. The four identified classified motions are: step forward (↑, the label "3"), step backward (↓, the label "4"), step left (←, the label "5"), and step right (→, the label "6"). The robot only has eight possible motion trajectories starting from its arbitrary initial state, given that there are only four motor imagery EEG control commands. An arc of 1/4 circle is adopted to interpolate the initial point and end point, which ensures the velocity vector remains tangent to the arc. If the step length of each motion is chosen appropriately and, this approximation trajectory for nonholonomic mobile system provides a collision-free path.

3.2.2. Trajectory tracking with ANFIS

If the controller has m inputs $(x_1, x_2, x_3, \cdots x_m)$ and one output y, the defined linguistic rules can be expressed as follows, where A_{ij} is a fuzzy set for the i-th rule and the j-th linguistic variable, and w_i is a real number that indicates its consequent part:

If x_1 is A_{i1} and x_2 is A_{i2} and $\cdots$ and x_m is A_{im}, Then y is w_i.

The Gaussian function is chosen as the membership function, given by Eq. (2). The output of the inference fuzzy system is computed by Eq. (3).

$$\mu_{ij} = e^{\frac{-(x_j - a_{ij})^2}{2b_{ij}^2}} \tag{2}$$

$$Y = \frac{\sum_{i=1}^{n} u_i w_i}{\sum_{i=1}^{n} u_i} \tag{3}$$

The value u_i represents the firing strength of each rule calculated by Eq. (4).

$$u_i = \mu_{i1}\mu_{i2}\cdots\mu_{im} \tag{4}$$

In the fuzzy controller presented above, define $z = (a_{11}, \cdots, a_{nm}, b_{11}, \cdots, b_{nm}, w_1, \cdots, w_n)$ the set of all parameters to be adapted in the neural network. Therefore, center values a_{ij} and width values b_{ij} of the Gaussian function and consequent values w_i must be adapted in order to achieve the necessary difference between desired output and actual output minimum. For example, take the wheeled robot as an example of the nonholonomic system. The function minimized for the position controller and orientation controller is represented by Eqs. (5) and (6) respectively [17].

$$V_p(t) = \sqrt{(x(t) - x^d(t))^2 + (y(t) - y^d(t))^2} \tag{5}$$

$$V_\theta(t) = (\theta(t) - \theta^d(t))^2 \tag{6}$$

$(x^d(t), y^d(t))$ represents the desired position and $\theta^d(t)$ represents the desired orientation of the nonholonomic robot, which are provided by the approximation trajectory in section 3.2.1. For the position controller and orientation controller respectively, the Godjevac algorithm is adopted to update the vector according to Eqs. (7)-(9). Γ_a, Γ_b and Γ_w are predefined constants.

$$a_{ij}(t+1) = a_{ij}(t) - \Gamma_a \times \frac{u_i}{\sum_{k=1}^{n} u_k}(y - y^d)(w_i - y)\frac{(x_j - a_{ij}(t))}{b_{ij}^2} \tag{7}$$

$$b_{ij}(t+1) = b_{ij}(t) - \Gamma_b \times \frac{u_i}{\sum_{k=1}^{n} u_k}(y - y^d)(w_i - y)\frac{(x_j - a_{ij}(t))}{b_{ij}^2} \tag{8}$$

$$w_i(t+1) = w_i(t) - \Gamma_w \times \frac{u_i}{\sum_{k=1}^{n} u_k}(y - y^d) \tag{9}$$

4. Experiment and validation

Our experiment utilized a two-wheeled robot as the typical nonholonomic system. The experiment was divided into two stages: the subject training stage and the nonholonomic robot control stage. The subject underwent a training session to master the coordination of motion direction with four classes of motor imagery EEG. Brain Products actiCHamp system with 32 electrodes was used to record EEG signals. In the robot control stage, the subject was exposed to a real scene with a Kheperal III robot and provided the motor imagery commands to generate collision-free motion planning for the robot.

4.1. Subject training stage

At the beginning of each training test, labeled “1”, a cross is projected on a screen for three seconds while the subject is in a relaxed state. A continuous sound stimulus is initiated at the second second, which indicates the upcoming experiment, and it is labeled “2”. Starting from the third second, four-direction arrows randomly appear on the screen for a duration of one second: forward (↑, the label "3"), stop (↓, the label "4"), left (←, the label "5"), and right (→, the label "6"). The subject imagines corresponding tongue, foot, left hand and right hand movements according to the prompts on the screen, for a duration of four seconds. There follows a one second pause, followed by a sound stimulus to indicate the end of the experiment. In order to prevent the overlap of two experiments and provide the subject some blinking and swallowing time, a 1.5-second blank time was reserved at the end. For the training stage, each experiment consisted of 16 minutes and 100 sets of data were

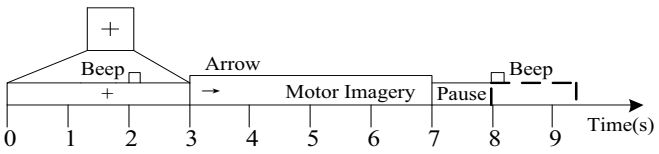

Fig. 1. Time sequence of experimental setup in subject training stage.

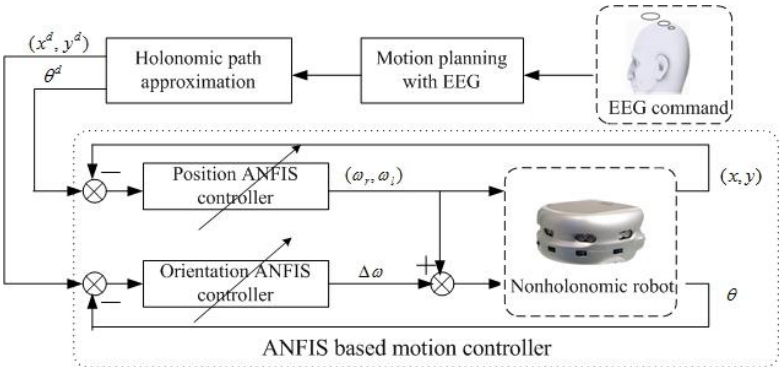

Fig. 2. Multi-level control strategy for nonholonomic robot.

collected. The experiment timing diagram is shown in Figure 1.

4.2. Nonholonomic robot control stage

4.2.1. ANFIS based controller

ANFIS is composed of a position and an orientation ANFIS controller allowing the robot to follow the desired collision-free path calculated from the holonomic path approximation. The planning of the holonomic path is implemented by the subject viewing the actual obstacle environment (Figure 2).

For the position controller, ANFIS is determined to contain five membership functions on its input, which are regularly distributed within $[-1,1]$ and are identical in width. There are three types of parameters to be adapted according to Eqs. (7)-(9): center values a_{ij}, width values b_{ij} and consequent values w_i The initial center values for each membership function are set to: $[a_{1j}(0), a_{2j}(0), a_{3j}(0), a_{4j}(0), a_{5j}(0)] = [-0.1, -0.05, 0, 0.05, 0.1]$. The corresponding initial width $b_{ij}(0) = 0.2$. The antecedent consequent value $w_i(0) = 0$. The predefined constants Γ_a, Γ_b and Γ_w, which influence the tracking speed and overshoot of the controller, are set to 1.00, 1.00 and 0.78 respectively.

For the orientation controller, ANFIS is also chosen to contain five membership functions which are regularly distributed within $[-\pi/8, \pi/8]$ and with the same width. The initial center values for each membership function are set to: $[a_{1j}(0), a_{2j}(0), a_{3j}(0), a_{4j}(0), a_{5j}(0)] = [-\pi/8, -\pi/16, 0, \pi/16, \pi/8]$. The corresponding width value $b_{ij}(0) = 0.3$. The antecedent consequent value $w_i(0) = 0$. The predefined constants Γ_a, Γ_b and Γ_w are chosen to be 1.00, 1.00 and 0.90 respectively.

4.2.2. Experiment results and analysis

It is notable that motor imagery of the foot corresponds to the motion of "turn $180°$ and stop" for the robot. In this case, the robot maneuvers in the opposite direction without stepping backward. Therefore, the robot can compensate its mistaken command recognition of the previous step immediately. The actual scene is designed to verify the performance of the proposed control strategy, as shown in Figure 3. A single-step prediction strategy is adopted for the subject to project the robot's motion one step in advance. The control strategy involves "conscious" motion planning by the subject and "unconscious" robot execution by neuron controller.

Suppose the ideal velocity of the Kephera III robot is set to 1.5 cm/s when it moves in a rectilinear line. For each motor imagery command, the operation of the robot lasts one step in duration, which

Fig. 3. Experimental setup in the robot control stage.

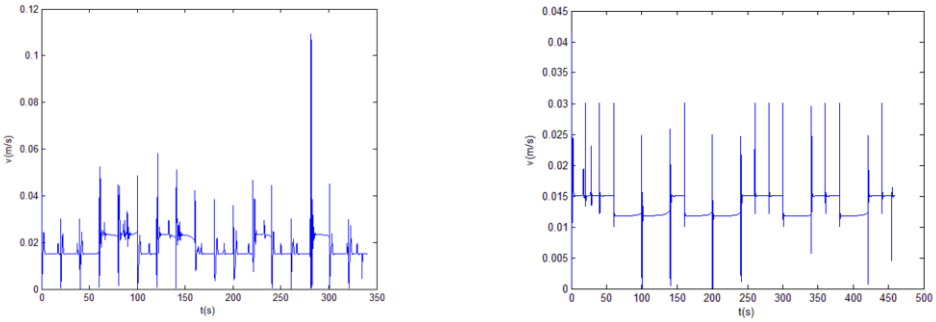

(a) Turning with a duration time of one step. (b) Turning with a duration time of two steps.

Fig. 4. Velocity scalar of robot for each step.

equates to 20 seconds. The velocity scalar of the robot for the fourth trial is listed in Figure 4(a), demonstrating that both the overshoot and velocity oscillations are very sharp when the robot makes a turn, if it receives a new command. By altering the duration of completion of the swerve to be twice that of a step, the subject can wait for the duration of a step when making their next prediction. The oscillation of velocity decreases dramatically when the robot makes a turn, as shown in Figure 4(b). Thus, the robot's locomotion is very smooth when responding to the new control command.

Results of five experimental trials are shown in Table 1. The first trial, for example, lasts 6.0 minutes and encompassed 18 control commands; all EEG signals were classified correctly with the exception of one motor imagery of the tongue, and one motor imagery of each the right hand and left hand, providing a total classification accuracy of 83.33%.

The fourth trial achieves the highest classification accuracy of 88.24%. It requires 17 EEG commands to control the robot from the initial position to the goal, as shown in Figure 5. The arrow indicates the planned motion for each step, and the associated number represents the label for the four classes of motor imagery EEG. For the fourth command in Trial 4, the motor imagery EEG of step forward is incorrectly classified as step left; because a single-step prediction is used, the robot had

Table 1

Control commands and classification accuracy of motor imagery EEG for five experimental trials.

Trial	Time	Total	Classification	Tongue	Foot	Left Hand	Right Hand
1	6.0	18	83.33%	11 (1)	0 (0)	4 (1)	3 (1)
2	7.0	20	80.00%	12 (2)	1 (0)	4 (1)	3 (1)
3	7.4	21	80.95%	14 (2)	1 (0)	3 (1)	3 (1)
4	5.8	17	88.24%	12 (1)	0 (0)	3 (0)	2 (1)
5	6.5	19	84.21%	10 (1)	2 (0)	3 (1)	4 (1)

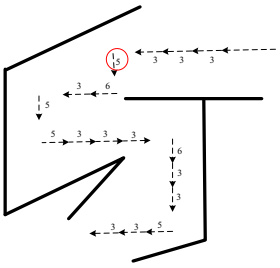

Fig. 5. Motor imagery command in the fourth trial.

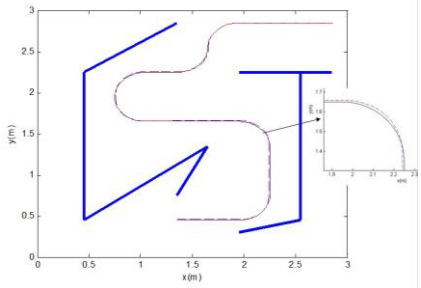

Fig. 6. Curvilinear motion trajectory based on ANFIS.

Fig. 7. Snapshot of actual robot motion trajectory.

already turned left when the fifth command was made. So, the subject made the step left command to correct the previous error.

The approximation of the holonomic robot's trajectory produced by motor imagery EEG is based on the method described in Section 3.2.1. The desired collision-free trajectory for the fourth experimental trial is shown as the continuous blue line in Figure 6. The parallel positions of the ANFIS controller and the orientation ANFIS controller are designed according to Section 3.2.2, in order to track the desired path. Without the necessity of advance training, the ANFIS controller can perform the control task while training. Therefore, the difference between the desired motion trajectory and real trajectory decreases with time, simultaneously improving the control accuracy. The curvilinear motion trajectory performed by the robot is presented as the red dashed line in Figure 6, demonstrating that the robot can follow the desired trajectory very quickly. Figure 7 displays the snapshots of the Khepera III robot motion trajectory with the proposed approach.

5. Conclusion

This paper proposed a new approach to increase the efficiency and control accuracy of nonholonomic mobile systems with an EEG-based BCI system, combinging the intelligence of human being and robot. This approach may be segmented into two parts: the first allows four classes of ERD/ERS based EEG to find a collision-free holonomic path, and the second is comprised of position and orientation controllers based on ANFIS to approximate the desired collision-free path. The advantage of this approach is that motion planning, which may be interpreted as conscious planning, is provided directly by human thoughts through motor imagery EEG. Moreover the nonholonomic mobile system operates in a reflexive way, through a fuzzy inference based adaptive controller. This approach realizes a multi-level control which allows the nonholonomic mobile system to change direction without stopping or relying on sensor information, thus increasing control precision and efficiency for the user.

Because the single-step prediction strategy was applied to plan the robot's motion, this would cause the subject to divide their attention, thereby influencing the recognized accuracy of ERD/ERS EEG signal. In future research, we will focus on combined non-brain based activities, such as eye-blinking, to improve the mapping between the robot's motion and control command.

Acknowledgment

This research has been made possible by "111 project" (Grant No.B13044) supported by the Ministry of Education of China.

References

[1] K. Choi and A. Cichocki, Control of a wheelchair by motor imagery in real time, Lecture Notes in Computer Science **5326** (2008), 330–337.
[2] R. Leeb, D. Friedman, G.R. Muller-Putz, R. Scherer, M. Slater and G. Pfurtscheller, Self-paced (asynchronous) BCI control of a wheelchair in virtual environ-ments: A case study with a tetraplegic, Computational Intelligence and Neuroscience **2007** (2007), 79642.
[3] C.S.L. Tsui and J.Q. Gan, Asynchronous BCI control of a robot simulator with supervised online training, Lecture Notes in Computer Science **4881** (2007), 125–134.
[4] D. Huang, K. Qian, D.Y. Fei, W. Jia, X. Chen and O. Bai, Electroencephalography (eeg)-based brain-computer interface (bci): A 2-d virtual wheelchair control based on event-related desynchronization/synchronization and state control, IEEE Transactions on Neural Systems Rehabilitation Engineering **20** (2012), 379–388.
[5] Y. Li, J. Long, T. Yu, Z. Yu, C. Wang, H. Zhang and C. Guan, An EEG-based BCI system for 2-D cursor control by combining Mu/Beta rhythm and P300 potential, IEEE Transactions on Biomedical Engineering **57** (2010), 2495–2505.
[6] J. Long, Y. Li, H. Wang, T. Yu, J. Pan and F. Li, A hybrid brain computer interface to control the direction and speed of a simulated or real wheelchair, IEEE Transactions on Neural Systems Rehabilitation Engineering **20** (2012), 720–729.
[7] H. Wang, Y. Li, J. Long, T. Yu and Z. Gu, An asynchronous wheelchair control by hybrid EEG–EOG brain–computer interface, Cognitive Neurodynamics **8** (2014), 399-409.
[8] B.H. Kim, M. Kim and S. Jo, Quadcopter flight control using a low-cost hybrid interface with EEG-based classification and eye tracking, Computers in Biology and Medicine **51** (2014), 82–92.
[9] S. Bhattacharyya, A. Sengupta, T. Chakraborti, D. Banerjee, A. Khasnobish, A. Konar, D.N. Tibarewala and R. Janarthanan, EEG controlled remote robotic system from motor imagery classification, In Proceedings of International Conference on Computing Communication & Networking Technologies, Coimbatore, 2012, pp. 1–8.
[10] J. Kronegg, G. Chanel, S. Voloshynovskiy and T. Pun, EEG-based synchronized brain–computer interfaces: A model for optimizing the number of mental tasks, IEEE Transactions on Neural System Rehabilitation Engineering **15** (2007), 50–58.
[11] R. Ron-Angevin, A. Dıaz-Estrella and F. Velasco-Alvarez, A two-class brain computer interface to freely navigate through virtual worlds, Biomed Tech **54** (2009), 126–133.
[12] F. Velasco-Alvarez, R. Ron-Angevin, L. da Silva-Sauer and S. Sancha-Ros, Audio-cued motor imagery-based brain-computer interface: Navigation through virtual and real environments, Neurocomputing **121** (2013), 89–98.
[13] J.D.R. Millan, F. Galan, D. Vanhooydonck, E. Lew, J. Philips and M. Nuttin, Asynchronous non-invasive brain-actuated control of an intelligent wheelchair, In Proceedings of IEEE International Conference on Engineering in Medicine and Biology Society, Minneapolis, 2009, pp. 3361–3364.
[14] K.T. Kim, T. Carlson and S.W. Lee, Design of a robotic wheelchair with a motor imagery based brain-computer interface, In Proceedings of International Winter Workshop on Brain-Computer Interface, Gangwo, 2013, pp. 46–48.
[15] B. Blankertz, G. Dornhege, G. Curio and K.R. Muller, Boosting bit rates in noninvasive EEG single-trial classification by feature combination and multiclass paradigms, IEEE Transactions on Neural Systems Rehabilitation Engineering **51** (2004), 993–1002.
[16] F. Jean, Complexity of nonholonomic motion planning, International Journal of Control **74** (2001), 776–782.
[17] T. Wang, F. Gautero, C. Sabourin and K. Madani, A neural fuzzy inference based adaptive controller for nonholonomic robots, International Journal of Computing **10** (2011), 56–65.